

International Congress of Science and Technology of Metallurgy and Materials, SAM -  
CONAMET 2013

## Measure of Zeta Potential of Titanium Pillared Clays

Sofía Zacur Vercellone<sup>a</sup>, Edgardo Sham<sup>a</sup>, Elsa Mónica Farfán Torres<sup>a\*</sup>

<sup>a</sup>INQUI, Universidad Nacional de Salta, Avenida Bolivia 5150, Salta 4400, Argentina

---

### Abstract

The change of the zeta potential,  $\zeta$ , with the pH as well as the isoelectric point of a charged particle are electrokinetic properties that characterize it. The  $\text{TiO}_2$  pillared clays are very interesting materials because of their ability to adsorb polluting substances and their potential to be used as photocatalyst in their degradation. That is why the preparation and characterization of these materials are important to improve their use in environmental chemistry. The aim of this work was the comprehension of the electrokinetic behavior of  $\text{TiO}_2$  pillared clays by the determination of  $\zeta$  and characterization of two  $\text{TiO}_2$  pillared clays and two  $\text{TiO}_2$  pillared organoclays prepared using different acid of hydrolysis, as well as in the original clay. The pillared organoclays presented a lower variation in the shape and the slope of the curves and in the IEP respect to that of the original clay. This behavior is due to the fact that the pillared organoclays has a lower content of pillars than that of the  $\text{TiO}_2$  pillared clays, because the alkylammonium cation blocks part of the available exchanging sites for the anchored of the  $\text{TiO}_2 \cdot x\text{H}_2\text{O}$  species. When these materials are calcined the number of negative charged sites neutralized by  $\text{TiO}_2$  will be minor than that observed for the pillared clays prepared in absence of surfactant. In consequence we can say that the preparation of  $\text{TiO}_2$  pillared clays using alkylammonium allows to obtain materials with a controlled superficial charge and porosity that can favor the access of polluting substances and their subsequent degradation in phototalytic treatments process.

© 2015 The Authors. Published by Elsevier Ltd. This is an open access article under the CC BY-NC-ND license (<http://creativecommons.org/licenses/by-nc-nd/4.0/>).

Selection and peer-review under responsibility of the scientific committee of SAM - CONAMET 2013

**Keywords:** pillared clays; organopillared clays; zeta potential

---

---

\* Corresponding author. Tel.: +54-0387-4255410; fax: +54-0387-4251006.

E-mail address: [mfarfan@unsa.edu.ar](mailto:mfarfan@unsa.edu.ar)

## 1. Introduction

Clays are attractive minerals for being used in adsorption and catalytic process. It has been proposed many methods to modify their properties to obtain materials with different characteristics (Zhou, 2010). The organic or inorganic cations introduction into laminar minerals like montmorillonite has been developed for preparing porous materials called pillared layered clays (PILCs). Some PILCs have pore openings of around 1 nm or even larger, which make them potential to serve as molecular sieves and selective catalysts. Various inorganic polyhydroxycations have been intercalated as pillaring precursors (Al, Ti, Ni, Zr, Fe, Cr, Mg, Cu, etc.) (Li et al., 2011). The pillared clays with TiO<sub>2</sub> pillars (TiO<sub>2</sub>-PILCs) have been used in catalytic degradation reactions of organic pollutant in water (Ooka et al., 2003; Ooka et al., 2004; Kun et al., 2006; Liu et al., 2007; Liu et al., 2009; Damardji et al., 2009; Abdennouri et al., 2011). Typically the TiO<sub>2</sub>-PILCs are obtained by adding a TiO<sub>2</sub> sol (prepared under acidic conditions) onto purified clay suspensions. The most active TiO<sub>2</sub> phase for catalysis is anatase. The surfactant addition during the TiO<sub>2</sub>-PILCs synthesis can promote the enhancement of the interlayer space and the introduction of titanium polyhydroxycations into deeper layers to get a homogeneous arrangement, which improves the TiO<sub>2</sub>-PILCs surface area. This fact also improves the pore distribution by the enhancement of the number of mesopores (Wang et. al., 2011). The zeta potential,  $\zeta$ , is one of the most important electrokinetic properties of clay minerals. This is an indicator of the potential magnitude at the beginning of the diffuse double layer of the particle. In many applications it is necessary to know the sign and magnitude of  $\zeta$  to estimate the colloidal dispersion stability, the particle affinity for certain substances, etc. For clays like montmorillonite,  $\zeta$  reminds practically constant (and negative) in a broad range of pH, which is typical for particles that have structural negative charge. This fact is independent of the ionic strength. Consequently, the electrokinetical potential is controlled by the permanent structural charges resulting from isomorphous substitution within the clay structure, which are independent of the external conditions. For montmorillonite, the contribution of variable (pH dependant) charges resulting from proton adsorption/ desorption reactions on the surface hydroxyl groups, at first, is negligible due to the fact that the edges represent 5%-10% of the total surface area (Avena and De Pauli, 1998; Duc et al., 2005). For organoclays, the  $\zeta$  net value diminishes, related to the raw clay. This probably happens due to the formation of inner-sphere complexes (Zacur et al. 2011).

The aim of the present work is the comprehension of the electrokinetic behavior of TiO<sub>2</sub> pillared clays by the determination of  $\zeta$  and characterization of two TiO<sub>2</sub> pillared clays and two TiO<sub>2</sub> pillared organoclays prepared using different acids of synthesis, as well as in the original clay.

### Nomenclature

$\zeta$	Zeta potential
PILCs	Pillared clays
TiO <sub>2</sub> -PILCs	Titanium oxide pillared clays
2MG	Purified clay
CEC	Cation exchange capacity
2MG-TiO <sub>2</sub>	Purified clay pillared with TiO <sub>2</sub>
2MG-TiO <sub>2</sub> HNO <sub>3</sub>	Purified clay pillared with TiO <sub>2</sub> synthesized with HNO <sub>3</sub>
2MG-TiO <sub>2</sub> CH <sub>3</sub> COOH	Purified clay pillared with TiO <sub>2</sub> synthesized with CH <sub>3</sub> COOH
HDTMA	hexadecyltrimetilammonium bromide
O2MG-TiO <sub>2</sub>	Purified clay pillared with TiO <sub>2</sub> synthesized with HDTMA
O2MG-TiO <sub>2</sub> HNO <sub>3</sub>	Purified clay pillared with TiO <sub>2</sub> synthesized with HNO <sub>3</sub> and HDTMA
O2MG-TiO <sub>2</sub> CH <sub>3</sub> COOH	Purified clay pillared with TiO <sub>2</sub> synthesized with CH <sub>3</sub> COOH and HDTMA

## 2. Materials and Methods

The raw clay was from “Dos Marias” mine placed in Chubut, Argentina. It belongs to a variety of montmorillonite called gray. Its cation exchange capacity (CEC) is 940 mmol/kg. The titanium (IV) tetraisopropoxide was provided by Aldrich Chemical Company, Inc. The nitric acid and the acetic acid were from Cicarelli. The surfactant (hexadecyltrimethylammonium bromide) was bought from Merk.

The raw clay was purified isolating the  $<2 \mu\text{m}$  sodium homoionic fraction according to standardized procedures.

### 2.1. Preparation of the Ti-pillaring solution

The Ti-pillaring solution was prepared by adding to 5M  $\text{HNO}_3$  a definite amount of 1M titanium (IV) tetraisopropoxide (isopropyl alcohol solution) in order to obtain a molar ratio  $\text{HNO}_3/\text{Ti} = 4$ . It was the same procedure with 5M  $\text{CH}_3\text{COOH}$ , in this case the final molar ratio was  $\text{CH}_3\text{COOH}/\text{Ti} = 10$ .

### 2.2. Synthesis of $\text{TiO}_2$ pillared clays (2MG- $\text{TiO}_2$ )

The  $\text{TiO}_2$  pillared clays were synthesized by adding the Ti-pillaring solution to a 1% purified clay suspension on stirring in order to reach 15mmol Ti/ g (clay). The mixture was stirred at 313K for 2 hours. The product was separated and washed with distilled water by centrifugation, and then was freeze drying. The resulting solid was calcined at 673K for 2 hours. The clay obtained after this procedure were called 2MG- $\text{TiO}_2$   $\text{HNO}_3$  and 2MG- $\text{TiO}_2$   $\text{CH}_3\text{COOH}$  depending on the acid used on the preparation of the Ti-pillaring solution.

### 2.3. Synthesis of $\text{TiO}_2$ pillared organoclays (O2MG- $\text{TiO}_2$ )

The  $\text{TiO}_2$  pillared organoclays were synthesized by adding a solution of hexadecyltrimethylammonium bromide (HDTMA) to a 1% purified clay suspension in order to obtain a HDTMA/CEC=0,5 ratio. The suspension was diluted to get a 0,2% concentration. The Ti-pillaring solution was added immediately until reaching the ratio  $\text{Ti}/\text{CEC} = 5$ . The mixture was stirred at 313K for 2 hour. Then the same procedure used for the synthesis of  $\text{TiO}_2$  pillared clays was followed. The clays obtained after this procedure were called O2MG- $\text{TiO}_2$   $\text{HNO}_3$  and O2MG- $\text{TiO}_2$   $\text{CH}_3\text{COOH}$  depending on the acid used in the Ti-pillaring solution preparation.

### 2.4. Characterization

The amount of titanium oxide was determined by chemical analysis for each sample, by titanium colorimetric determination (Sandell, 1950). X Ray Diffraction (XRD) patterns were obtained using a RIGAKU-DENKI D-Max IIC powder diffractometer with a  $\text{Cu-K}\alpha$  emission of 40V. The samples were analyzed by FTIR using a Spectrum GX Perkin Elmer (as KBr pellets) in the range of  $400 \text{ cm}^{-1}$ - $4000 \text{ cm}^{-1}$ . Surface areas and pore size distributions were determined using nitrogen as the sorbate at 77K in a Micromeritics ASAP 2020 analyzer. Zeta potential measurements were performed using a Zeta- Meter System 3.0+, the ionic strength was adjusted with  $10^{-2}\text{M}$   $\text{KNO}_3$  and the pH was modified by adding  $10^{-1}\text{M}$  KOH and  $10^{-1}\text{M}$   $\text{HNO}_3$  solutions.

## 3. Results and discussion

Table 1 shows the titania content determined for each sample. Fig. 1 shows the XRD patterns of the samples. It can be seen the low cristallinity of all materials (a,b,c,d), the which implies a high disperse  $\text{TiO}_2$  phase. The diffraction lines at  $2\theta = 25,2$  and  $2\theta = 48,0$  are observed in all samples, except for the purified clay. These diffraction lines correspond to anatase phase. Other characteristic anatase diffraction lines (for example  $2\theta = 54,9$ ) may be overlapped with montmorillonite characteristic lines. The basal diffraction line (001) only appears for the purified clay at  $2\theta = 6,99$ .

Table 1. Titania content

Sample	% Ti	% TiO <sub>2</sub>
O2MG-TiO <sub>2</sub> CH <sub>3</sub> COOH	7,7	12,9
O2MG-TiO <sub>2</sub> HNO <sub>3</sub>	8,3	13,8
2MG-TiO <sub>2</sub> HNO <sub>3</sub>	13,2	22,1
2MG-TiO <sub>2</sub> CH <sub>3</sub> COOH	15,3	25,6

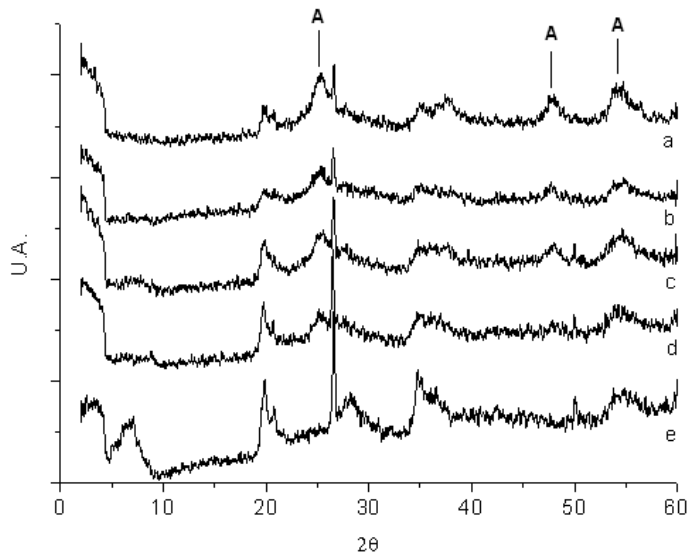
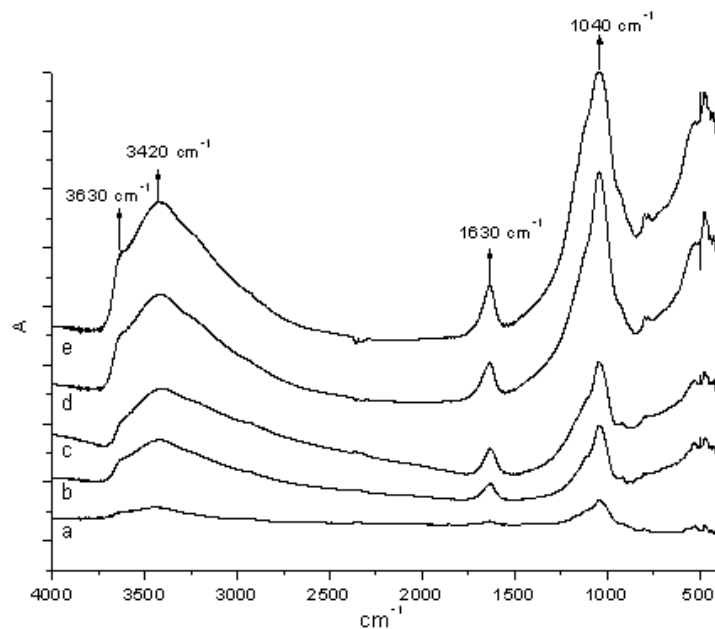
Fig.1. XRD patterns. a) 2MG-TiO<sub>2</sub> HNO<sub>3</sub>. b) 2MG-TiO<sub>2</sub> CH<sub>3</sub>COOH. c) O2MG-TiO<sub>2</sub> HNO<sub>3</sub> d) O2MG-TiO<sub>2</sub> CH<sub>3</sub>COOH e) 2MG.Fig.2. FT-IR spectra. a) 2MG b) 2MG-TiO<sub>2</sub> HNO<sub>3</sub> c) 2MG-TiO<sub>2</sub> CH<sub>3</sub>COOH d) O2MG-TiO<sub>2</sub> HNO<sub>3</sub> e) O2MG-TiO<sub>2</sub> CH<sub>3</sub>COOH

Table 2. Relative intensities for the bands at 1630  $\text{cm}^{-1}$  ( $\text{H}_2\text{O}$ ) and 3420  $\text{cm}^{-1}$  ( $-\text{OH}$ )

Sample	$\text{H}_2\text{O}/\text{Si-O}$	$-\text{OH}/\text{Si-O}$
2MG	0,87	0,96
2MG- $\text{TiO}_2$ $\text{HNO}_3$	0,75	0,94
2MG- $\text{TiO}_2$ $\text{CH}_3\text{COOH}$	0,60	0,91
O2MG- $\text{TiO}_2$ $\text{CH}_3\text{COOH}$	0,50	0,70
O2MG- $\text{TiO}_2$ $\text{HNO}_3$	0,48	0,66

The diffuse XRD pattern observed for pillared clays and pillared organoclays indicates a highly disordered structured which is referred to as “delaminated clays” by some articles (Yuan et al., 2006; Chen et al., 2012).

Fig.2 shows FT-IR spectra of the purified clay, pillared clays samples and pillared organoclays samples. A weak band at near 3630  $\text{cm}^{-1}$  is due to stretching vibrations of  $\text{Al-OH}$  and a strong broad band at 3420  $\text{cm}^{-1}$  can be attributed to the stretching vibration of the hydroxyl group and the interlayer water molecules. On pillaring this band broadens due to the introduction of more  $\text{OH-}$  groups of the pillars, which is interpreted as an effect of pillaring (Kurian and Sugunan, 2003). The band near of 1630  $\text{cm}^{-1}$  is also the bending vibration of the hydroxyl and interlayer water molecules. The strong band at 1040  $\text{cm}^{-1}$  is assigned to  $\text{Si-O}$  stretching vibration. The Table 2 shows the reduction of the intensity ratio between the band at 3420  $\text{cm}^{-1}$  (or 1630  $\text{cm}^{-1}$ ) and the band at 1040  $\text{cm}^{-1}$ . The decrease in intensity arises from the dehydration and dehydroxylation steps during pillaring. Pillaring process replace large amount of interlayer cations that generally exists as hydrated. In addition pillared clay has low amount of adsorbed/ coordinated water due to the non- swellable nature (Ouidri and Kha, 2009). In addition the broad band at 600-900  $\text{cm}^{-1}$  can be assigned to the characteristic IR absorption band of crystalline  $\text{TiO}_2$  and montmorillonite itself (Liu et al., 2007).

Fig. 3 and 4 represent adsorption / desorption isotherms and pore size distribution for the pillared clays, the pillared organoclays and the purified clay. They belong to Type IV in the Brunauer, Deming, Deming and Teller (BDDT) classification corresponding to a mesoporous structure. The specific surface area was calculated by the BET equation ( $S_{\text{BET}}$ ) and the total pore volume (TPV) was evaluated from nitrogen uptake at a relative pressure of 0,98. The t-plot according to Harkins-Jura-Boer method was used to calculate the micropore volume ( $V_{\mu\text{P}}$ ) and the external surface area ( $S_{\text{EXT}}$ ). The Barret-Joyner-Halenda (BJH) method was used to evaluate the average pore diameter ( $w_p$ ). These structural parameters are summarized in Table 3. The BET surface area and the external surface area for all pillared clays and pillared organoclays are bigger than those of the purified clay. The micropore volume has diminished for pillared clays and pillared organoclays compared to the purified clay. The samples synthesized using  $\text{HNO}_3$  has a bigger BET surface area than those synthesized with  $\text{CH}_3\text{COOH}$  probably because the last ones went through a slower hydrolysis process and formed smaller  $\text{TiO}_2$  pillars. However the TPV almost has no changes and the incorporation of a surfactant reduce the BET surface area. It might be due to the fact that once the surfactant molecules are burned off, pore collapses could happen in the region where there are no pillars, leading to a decrease in the total surface area, or because the incomplete removal of carbon residues in the calcinations procedure blocks the pores of the samples.

Table 3. Structural parameters

Sample	$S_{\text{BET}}$ ( $\text{m}^2/\text{g}$ )	TPV ( $\text{cm}^3/\text{g}$ )	$V_{\mu\text{P}}$ ( $\text{cm}^3/\text{g}$ )	$S_{\text{EXT}}$ ( $\text{m}^2/\text{g}$ )	$w_p$ (nm)
2MG- $\text{TiO}_2$ $\text{HNO}_3$	263	0,258	-0,006	62	3,06
O2MG- $\text{TiO}_2$ $\text{HNO}_3$	203	0,230	0,010	105	3,70
2MG- $\text{TiO}_2$ $\text{CH}_3\text{COOH}$	202	0,258	0,010	100	4,51
O2MG- $\text{TiO}_2$ $\text{CH}_3\text{COOH}$	197	0,263	0,010	94	4,48
2MG	110	0,258	0,019	31	3,89

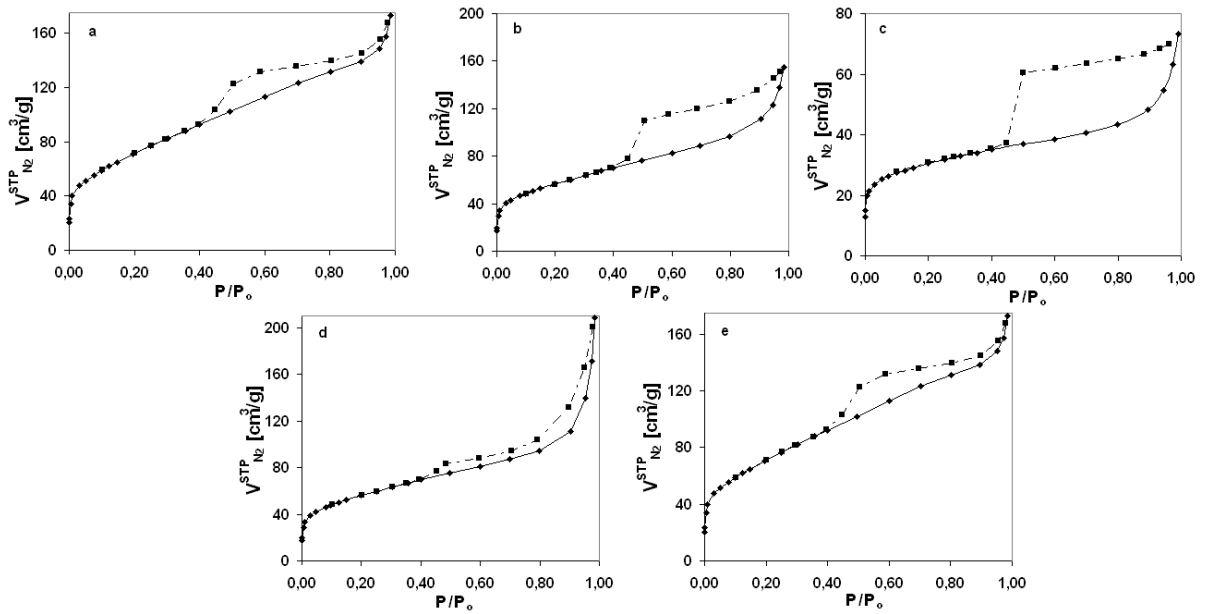


Fig 3. Nitrogen adsorption/ desorption isotherms. a) 2MG-TiO<sub>2</sub> HNO<sub>3</sub> b) O2MG-TiO<sub>2</sub> HNO<sub>3</sub> c) 2MG d) 2MG-TiO<sub>2</sub> CH<sub>3</sub>COOH e) O2MG-TiO<sub>2</sub> CH<sub>3</sub>COOH

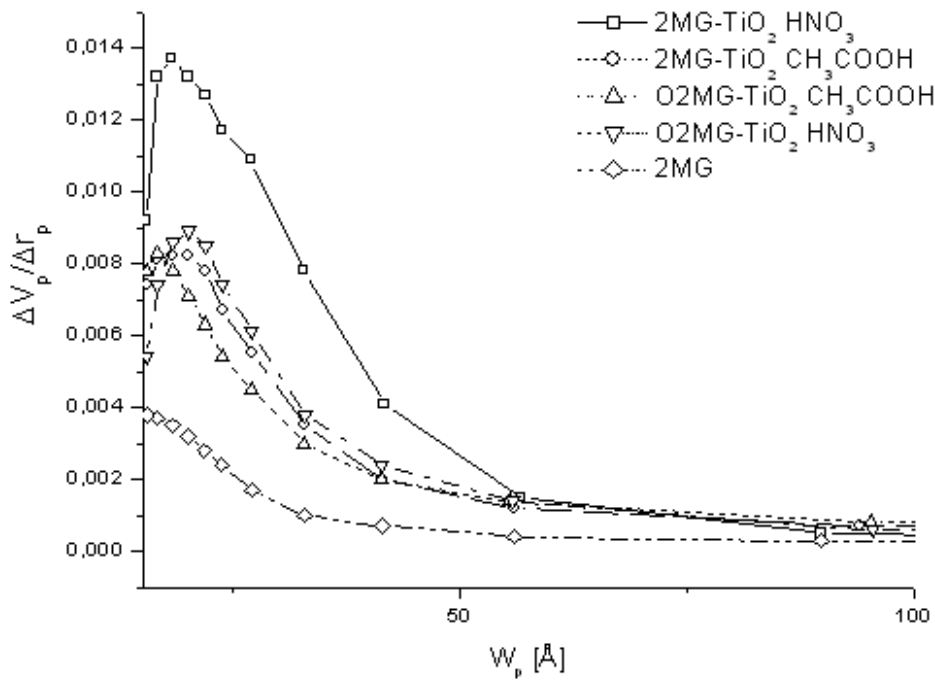


Fig 4. Pore size distribution

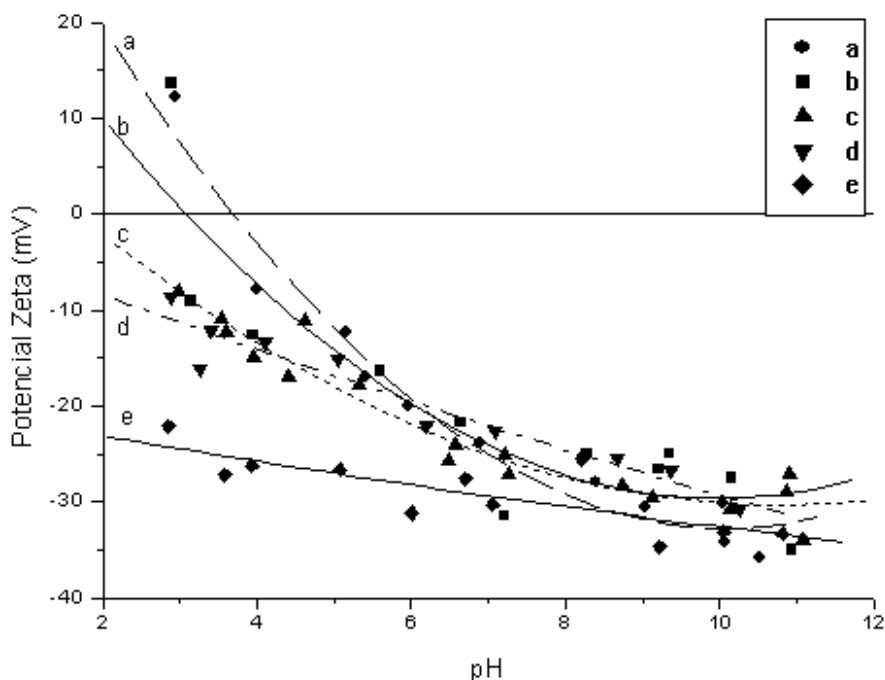


Fig. 5  $\zeta$  vs. pH. a) 2MG-TiO<sub>2</sub> CH<sub>3</sub>COOH. b) 2MG-TiO<sub>2</sub> HNO<sub>3</sub>. c) O2MG-TiO<sub>2</sub> HNO<sub>3</sub>. d) O2MG-TiO<sub>2</sub> CH<sub>3</sub>COOH. e) 2MG.

The  $\zeta$  determination results are shown on Fig 5. The approximate isoelectric points (IEP) for each sample are detailed in Table 4. It can be seen that the IEP changed for the pillared clays and the pillared organoclays compared to the original clay. The shape of the curves is also different, exhibiting a greater variation of  $\zeta$  with the pH. In the original clay (2MG)  $\zeta$  remains practically constant in the studied pH range, which is expected for particles that have structural negative charges resulting from isomorphous substitution. The purified clay (2MG) and the samples O2MG-TiO<sub>2</sub> (especially those synthesized with acetic acid) are negatively charged in the pH studied range. It also can be seen that the increasing TiO<sub>2</sub> content order is coincident with the increasing order for the IEP: 2MG < O2MG-TiO<sub>2</sub> CH<sub>3</sub>COOH < O2MG-TiO<sub>2</sub> HNO<sub>3</sub> < 2MG-TiO<sub>2</sub> CH<sub>3</sub>COOH < 2MG-TiO<sub>2</sub> HNO<sub>3</sub>.

The TiO<sub>2</sub> pillared organoclays (O2MG-TiO<sub>2</sub>) has a lower content of pillars because the alkylammonium cation blocks part of the available exchanging sites for the anchored of the TiO<sub>2</sub>.xH<sub>2</sub>O species. When these materials are calcined, the alkylammonium is eliminated, releasing the exchanging sites. In this way, the number of negative charged sites neutralized by TiO<sub>2</sub> will be minor than for the pillared clays prepared in absence of surfactant (2MG-TiO<sub>2</sub>). In these last ones, the  $\zeta$  variation with the pH is bigger, showing a greater contribution of variable charges. In the Fig. 6 is shown a schematic representation of the TiO<sub>2</sub> pillared clays and the TiO<sub>2</sub> pillared organoclays.

Table 4. Isoelectric points

Sample	pH for the IEP
2MG-TiO <sub>2</sub> HNO <sub>3</sub>	3
2MG-TiO <sub>2</sub> CH <sub>3</sub> COOH	3,7
O2MG-TiO <sub>2</sub> HNO <sub>3</sub>	1,7
O2MG-TiO <sub>2</sub> CH <sub>3</sub> COOH	-0,8
2MG	-11,9

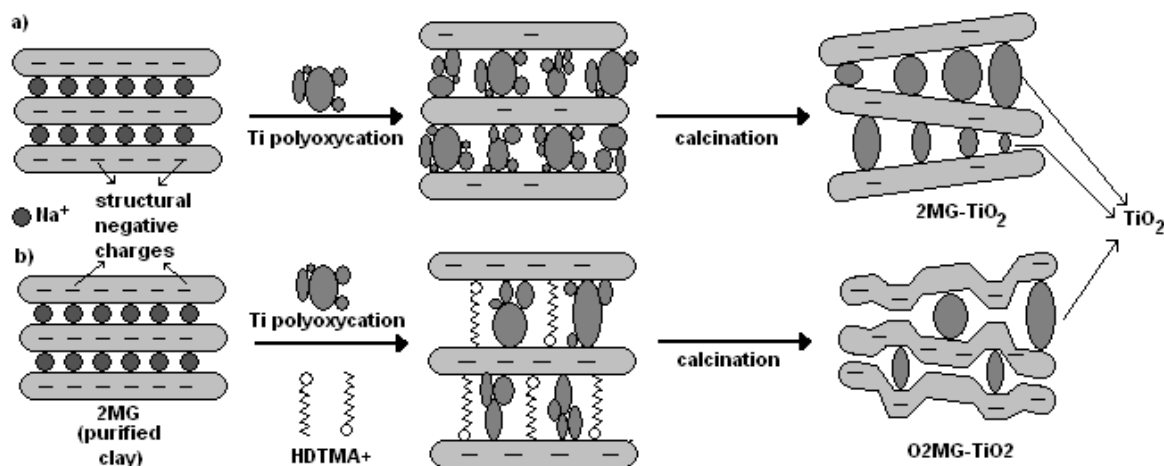


Fig.6 Schematic representation. a) TiO<sub>2</sub> pillared clays (2MG-TiO<sub>2</sub>). b) TiO<sub>2</sub> pillared organoclays (O2MG-TiO<sub>2</sub>).

#### 4. Conclusions

The TiO<sub>2</sub> pillared clays and the TiO<sub>2</sub> pillared organoclays were synthesized and characterized. Measures of  $\zeta$  were performed on them. It could be seen differences in the shape of the curves  $\zeta$  vs. pH for all the samples. No substantial differences could be observed in the electrokinetic behavior between samples synthesized with different acids, although they had different structural properties. Different IEP were found between samples synthesized with and without surfactant addition. This could be explained by the fact that for the O2MG-TiO<sub>2</sub> the number of negative charged sites neutralized by TiO<sub>2</sub> is minor than for the 2MG-TiO<sub>2</sub>, then the pillars density is also lower. In consequence we can say that the preparation of TiO<sub>2</sub> pillared clays using alkylammonium allows to obtain materials with a controlled superficial charge and porosity that could favor the access of some polluting substances and their subsequent degradation in photocatalytic treatments process.

#### References

- Abdennouri M., Baálala M., Galadi A., El Makhfouk M., Bensitel M., Nohair K., Sadiq M., Boussaoud A., Barka N., 2011. Photocatalytic degradation of pesticides by titanium dioxide and titanium pillared purified clays. *Arabian Journal of Chemistry*, doi:10.1016/j.arabjc.2011.04.005.
- Avena M. J., De Pauli C. P., 1998. Proton Adsorption and Electrokinetics of an Argentinean Montmorillonite. *Journal of Colloid and Interface Science* 202, 195-204.
- Chen D., Zhu Q., Zhou F., Deng X., Li F., 2012. Synthesis and photocatalytic performances of the TiO<sub>2</sub> pillared montmorillonite. *Journal of Hazardous Materials* 235–236, 186–193.
- Damardji B., Khalaf H., Duclaux L., David B., 2009. Preparation of TiO<sub>2</sub>-pillared montmorillonite as photocatalyst Part II: Photocatalytic degradation of a textile azo dye. *Applied Clay Science* 45, 98-104.
- Duc M., Gaboriaud F., Thomas F., 2005. Sensitivity of the acid–base properties of clays to the methods of preparation and measurement: 1. Literature review. *Journal of Colloid and Interface Science* 289, 139-147.
- Kun R., Mogyorósi K., Dékány I., 2006. Synthesis and structural and photocatalytic properties of TiO<sub>2</sub>/ montmorillonite nanocomposites. *Applied Clay Science* 32, 99-110.
- Kurian M., Sugunan S., 2003. Liquid phase benzylation of o-xylene over pillared clays. *Indian Journal of Chemistry* 42A, 2480-2486.
- Li X., Lu G., Qu Z., Zhang D., Liu S., 2011. The role of titania pillar in copper-ion exchanged titania pillared clays for the selective catalytic reduction of NO by propylene. *Applied Catalysis A: General* 398, 82-87.
- Liu J., Li X., Zuo S., Yu Y., 2007. Preparation and photocatalytic activity of silver and TiO<sub>2</sub> nanoparticles/ montmorillonite composites. *Applied Clay Science* 37, 275-280.
- Liu J., Dong M., Zuo S., Yu Y., 2009. Solvothermal preparation of TiO<sub>2</sub>/montmorillonite and photocatalytic activity. *Applied Clay Science* 43, 156-159.



- Ooka C., Yoshida H., Horio M., Suzuki K., Hattori T., 2003. Adsorptive and photocatalytic performance of TiO<sub>2</sub> pillared montmorillonite in degradation of endocrine disruptors having different hydrophobicity. *Applied Catalysis B: Environmental* 41, 313-321.
- Ooka C., Yoshida H., Suzuki K., Hattori T., 2004. Highly hydrophobic TiO<sub>2</sub> pillared clay for photocatalytic degradation of organic compounds in water. *Microporous and Mesoporous Materials* 67, 143-150.
- Ouidri S., Kha H., 2009. Synthesis of benzaldehyde from toluene by a photocatalytic oxidation using TiO<sub>2</sub>-pillared clays. *Journal of Photochemistry and Photobiology A: Chemistry* 207, 268–273.
- Sandell E.B., 1950. *Colorimetric Determination of Traces of Metals*. Interscience Publishers, Inc., Nueva York, pp. 572-576.
- Yuan P., Yin X., He H., Yang D., Wang L., Zhu J., 2006. Investigation on the delaminated-pillared structure of TiO<sub>2</sub>-PILC synthesized by TiCl<sub>4</sub> hydrolysis method. *Microporous and Mesoporous Materials* 93, 240–247.
- Wang Q., Liu Z., Zou H., Zhao Z., Wei X., 2011. Effect of surfactant modification on the desulfurization performance of Zn/Ti-PILCs adsorbent. *Journal of Fuel Chemistry and Technology* 39, 203-206.
- Zacur S.S., Naranjo P.M., Farfán E.M., 2011. Organoarcillas: Propiedades electrocinéticas y estructura. *Anales XVII Congreso Argentino de Físicoquímica*, Córdoba, Argentina.
- Zhou C.H., 2010. Emerging trends and challenges in synthetic clay-based materials and layered double hydroxides. *Applied Clay Science* 48, 1-4.